

Photochemical Synthesis of (2E,4Z)-5-(anthracen-9-yl)-2-cyanopenta-2,4-dienamide

Rabih O. Al-Kaysi ^{1,*}, Imadul Islam ¹, Raghad Al-Muzarie ¹, and Christopher J. Bardeen ²

¹ College of Science and Health Professions, King Saud bin Abdulaziz University for Health Sciences, and, King Abdullah International Medical Research Center (Nanomedicine), Ministry of National Guard Health Affairs, Riyadh 11426, Kingdom of Saudi Arabia.

² Department of Chemistry, University of California, Riverside, Riverside, CA 92521, USA.

* Correspondence: kaysir@ksau-hs.edu.sa; Tel.: +966561429528

Abstract: In this short note we describe the photochemical synthesis of (2E,4Z)-5-(anthracen-9-yl)-2-cyanopenta-2,4-dienamide (**4**) from the corresponding (2E,4E)-5-(anthracen-9-yl)-2-cyanopenta-2,4-dienamide (**3**) and subsequent purification by precipitation from aqueous surfactant. Compound like **4** belongs to a family of anthracene derivatives capable of forming crystals that can photo-mechanically deform with light. Synthesis of **3** was achieved with high yields and in less than one minute via secondary amine-catalyzed Knoevenagel condensation between commercially available (E)-3-(anthracen-9-yl)acrylaldehyde (**1**) and 2-cyanoacetamide (**2**). Photochemical conversion of a solution of the **3** in acetonitrile using light > 475 nm from a commercial blue LED leads to a mixture of **4** (87%) and unconverted **3** (13%) due to the presence of a photostationary state from overlapping absorption spectral regions. Pure **4** (>99%) was later obtained by precipitating an organic solution of the photoproduct from aqueous surfactant Sodium Dodecyl Sulfate (SDS). Pure **4** was collected in the form of acicular micro crystals that are photomechanically responsive to UV light. The products were analyzed using ¹H NMR, ¹³C NMR, IR, UV-Vis, and HPLC.

Keywords: Knoevenagel condensation, Anthracene, Photochemical, Photomechanical.

Introduction

Photo-mechanical molecular crystals are an emerging class of smart materials that can convert UV or visible light to mechanical motion of the crystal[1,2]. Our group has pioneered the use of photomechanical crystals made from anthracene derivatives as the photo-harvesting chromophore[3–7]. To achieve diversity in photomechanical responses like bending[8,9], peeling[10,11], jumping[12,13], etc. different analogs of anthracene derivatives were synthesized and tested (Figure 1).

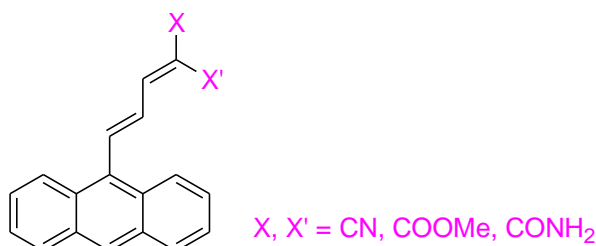


Figure 1: General chemical structure of anthracene derivatives that are photomechanically active as crystals.

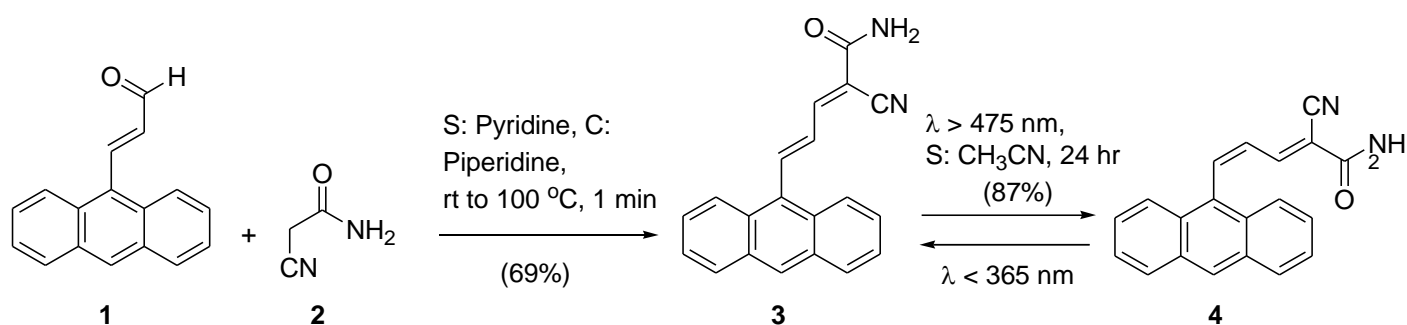
In this short note, we describe the photochemical synthesis of (2E,4Z)-5-(anthracen-9-yl)-2-cyanopenta-2,4-dienamide **4** from (2E,4E)-5-(anthracen-9-yl)-2-cyanopenta-2,4-dienamide (**3**).

Results and Discussion

To achieve the synthesis of the title compound **4**, the reaction depicted in Scheme-1 was followed. The starting materials **1** and **2** were readily available from commercial sources such as TCI, Sigma-Aldrich, or Santa Cruz Biotechnology. However, due to the rising cost of reagents and global inflation derivatives such as **1** have been discontinued, or increased in retail price. However, compound **1** can be conveniently synthesized using Mizoroki–Heck reaction between 9-bromanthracene and acrolein diethyl acetal using palladium acetate as a catalyst between **1** and excess of **2** in Pyridine solvent and piperidine as the catalyst yields compound **3** in high yields. Although the use of Pyridine is undesirable due to its potential health hazards, the amount of solvent used was small relative to the amount of reactants. The use of a catalyst such as piperidine is crucial for the reaction to proceed with a high yield. When the reactants are dissolved in pyridine, a faint yellow color solution forms with no product formation as indicated by TLC analysis, silica gel 50%:50% Ethyl acetate, hexane mobile phase. When a catalytic amount of piperidine is added the reaction mixture immediately turns red color indicating product formation. The reaction can be accelerated by heating to 100 °C for less than 1 minute. If piperidine was unavailable, morpholine or a secondary amine works just as well as a catalyst. Using excess 2-cyanoacetamide (**2**) ensures the complete conversion of the more expensive starting material **1** and simplifies subsequent purification steps. The excess 2-cyanoacetamide can be easily washed away with water or efficiently removed from the product via crystallization from acetonitrile/ water mixture. The Knoevenagel condensation affords the thermodynamically more stable trans or in this case E-isomer of **4**. An analogous reaction between trans-cinnamaldehyde and 2-cyanoacetamide affords the E,E-isomer in high yields [19].

Compound **3** was obtained in pure E,E-isomeric form with a chemical yield close to 69%. The purity of the product was confirmed using HPLC, ¹H, and ¹³C NMR. HPLC chromatogram showed the elution of one peak with a retention time comparable to small molecules with similar chemical structures (Supplementary Figure 7). The UV-Vis spectrum of **3** in acetonitrile (Supplementary Figure 5) has a broad maximum absorption around 430 nm indicative of the intramolecular charge-transfer character of these derivatives[9][20]. The title compound **4** was photochemically prepared by the photolysis of a solution of **3** in a polar aprotic solvent such as acetonitrile. In a typical photochemical synthesis, a solution of **3** in acetonitrile was purged with argon gas and photolyzed for one day using light from a commercial blue LED strip having a maximum output at 475 nm. Removal of the solvent under reduced pressure affords a mixture containing roughly 87% **4** with remaining unconverted **3** as was revealed by ¹H NMR and HPLC analysis (Supplementary Figure 15). No secondary photoproducts were detected. Incomplete conversion of **3** to **4** was due to overlapping absorption spectra of both compounds in the region between 450-475 nm where the charge-transfer band is dominant (Supplementary Figure 17). This spectral overlap reduces conversion to **4** to less than 100%. This is typical for such anthracene derivatives as was previously shown for similar derivatives [7,10]. We could not separate **3** and **4** using column chromatography or prep-TLC due to their overlapping R_f values. Recrystallization from co-solvents did not improve the isomeric ratio of **4** to **3**. More sophisticated techniques such as prep-HPLC must be employed instead. Unfortunately, not all research groups are equipped with such a specialized instrument. However, when a concentrate solution (0.2 molar) of the 87% **3** in N,N-DMF was injected in a warm solution of 0.025 Molar aqueous SDS and was allowed to stand at 45 °C for 24 hours, crystalline microwires of pure **4** separate with roughly 99.7% purity, determined by HPLC (Supplementary Figure 14) and ¹H NMR analysis (Supplementary Figure 8, 9).

For compound **3**, photochemical isomerization occurs at the double bond adjacent to the anthracene ring as was previously observed for similar analogs[4,7,9,21,22]. The J-coupling constant of the proton on carbon-16 (δ_H 7.11 ppm) in **3** has a value of 15.5 Hz, typical for an E-geometrical configuration. In compound **4** the coupling constant on carbon-16 (δ_H 7.19 ppm) drops down to 11.8 Hz, typical for the Z-geometric configuration. The chemical shift of the amine protons is inequivalent which was unexpected given the symmetry of the amide group. However, an ¹H NMR of the 2-cyanoacetamide (**2**) [23] in a similar deuterated solvent shows that the two amide hydrogens are indeed inequivalent appearing as two broad singlets with a chemical shift around 7-8 ppm. This chemical inequivalence was observed with N,N-DMF where the two methyl groups appear as two singlets.



Scheme 1. Synthesis of **3** and **4**. Irradiation of **4** at 365 nm regenerates only 55% of **4** (Supplementary Figure 16)

Materials and Methods

All the organic solvents used were a reagent grade. Spectroscopic grade solvents were used as received. Thin layer chromatography (TLC) was performed on 5x2.5 cm pre-coated silica gel GF₂₅₄ on an aluminum sheet. Spots on TLC were visualized using UV light (254 nm) or developed chemically using KMnO₄ solution. Reagents such as (E)-3-(anthracen-9-yl)acrylaldehyde and 2-cyanoacetamide were purchased from TCI America and Santa Cruise Biotechnology and were used without further purification. ¹H and spectra were recorded on JEOL (400 MHz) at 298 K. Abbreviations were used to describe peak splitting patterns: s = singlet, d = doublet, dd = doublet of doublet, ddd = doublet of doublet of doublet, m = multiplet. ¹³C NMR spectra were recorded JEOL at (100 MHz) spectrometer with complete proton decoupling at 298 K. Proton chemical shifts were reported in ppm (δ) (DMSO-*d*₆, δ 2.50 ppm) and *J* values are reported in hertz (Hz). Carbon chemical shifts were reported in ppm (δ) (DMSO-*d*₆, δ 39.52 ppm). A 33% (V/V) mixture of DMSO-*d*₆ in CCl₄ was used instead of pure DMSO-*d*₆ to increase the solubility of the compound and prevent the solution from freezing. IR measurements were performed on an IR Affinity-1 FTIR from Shimadzu. A sample (~1%) was pulverized with spectroscopic grade KBr and pressed into a transparent pellet. High Performance Liquid Chromatography (HPLC) analysis was performed on a Shimadzu (LC-20AD) using a Thermo Scientific general purpose BDS Hypersil C18 column (250 × 4.6 mm dimensions) held at a constant temperature of 35 °C. A gradient mobile phase was used starting with 50% aqueous acetonitrile in water (pH = 2.5) and finishing with 100% acetonitrile at a flow rate of 1.5 mL/min. The detector wavelength was set to 254 nm. UV analysis was performed on Spectro UV-Vis (UVD 2950) from Labomed Inc with a 1 cm quartz cell and a slit width of 1.0 nm. The wavelength range was selected between 200-600 nm. A solvent blank was collected before each measurement. Melting points (uncorrected) were measured on a 1101D Mel-Temp digital melting point apparatus

Synthesis:

(2E,4E)-5-(anthracen-9-yl)-2-cyanopenta-2,4-dienamide (**3**): The following synthesis was performed under dim light or inside an Amber-colored vial. A reaction vial with 40 mL capacity was charged with (E)-3-(anthracen-9-yl)acrylaldehyde **1** (0.232 g, 1mmol, 1 equivalent) and 2-cyanoacetamide (0.21 g, 2.5 mmol, 2.5 equivalent). The reactants were dissolved in 4 ml of dry pyridine then piperidine (0.025 ml, 0.25 mmol, ¼ mole equivalent) was added and the reaction was stirred at 100 °C for roughly 4 minutes or till the (E)-3-(anthracen-9-yl)acrylaldehyde was consumed. The reaction progress was monitored by TLC using activated silica gel ad 50%/50% by volume of ethyl acetate and hexane (R_f = 0.22 for **3** and R_f = 0.53 for reactant **1**). The reaction was cooled to room temperature followed by adding 40 ml of DI water to precipitate the orange product **3** which was suction filtered and washed with copious amounts of DI water

to remove pyridine and excess 2-cyanoacetamide. The product was recrystallized from boiling acetonitrile triturated with boiling water to obtain orange needle-like long crystals with a 69% yield (0.21 g). Mp 226-228 °C . IR $\nu_{\max}/\text{cm}^{-1}$ 3395 (strong), 3171 (medium), 2225 (weak, cyano stretch), 1709 (strong, CO stretch), 1395 (strong, C-N stretch) (**Supplementary Figure 6**). ^1H NMR (400 MHz, DMSO- D_6) δ_{H} 8.54 (s, 1H), 8.40 (d, $J = 15.5$ Hz, 1H), 8.31 (dd, $J = 14.6$, 10.0 Hz, 3H), 8.05 (d, 2H), 7.71 – 7.39 (m, 6H), 7.11 (dd, $J = 15.5$, 11.4 Hz, 1H) (**Supplementary Figure 1, 2**); ^{13}C NMR (101 MHz, DMSO- D_6) δ_{C} 161.94, 151.13, 143.29, 131.92, 131.01, 129.67, 129.20, 128.80, 128.49, 126.43, 125.24, 124.90, 115.07, 108.58 (**Supplementary Figure 3, 4**)

(2*E*,4*Z*)-5-(anthracen-9-yl)-2-cyanopenta-2,4-dienamide (**4**): Into a 100 mL round-bottom Schlenk flask was added (2*E*,4*E*)-5-(anthracen-9-yl)-2-cyanopenta-2,4-dienamide (0.1 g, 0.33 mmol) and dissolved in 60 ml of dry acetonitrile. The solution was purged with Argon gas for several minutes and then placed in the middle of a loop containing a blue LED strip with a wavelength output between 450 and 500 nm matching the absorption spectrum of the **3** in acetonitrile. The solution was stirred making sure the reaction does not warm up by maintaining proper ventilation. After 3 days of photolysis, the solvent was removed under reduced pressure to yield a yellow solid that was used without further purification. The product contained roughly 85% compound **4** with 15 % unconverted **3**. No other side products were detected as evident from the HPLC analysis. To obtain pure **4**, a 20 mg of the crude product was dissolved in 0.4 ml of *N,N*-DMF before rapidly being injected in 20 ml of warm (45 C) aqueous SDS solution (0.025 molar). The mixture was allowed to rest undisturbed at 45 C for 24 hours until pure crystals of **4** precipitated out of the solution. The crystals were suction filtered and washed with DI water. Obtained yellow fine crystal with 65 % yield (11 mg). Mp 221-223 °C. IR $\nu_{\max}/\text{cm}^{-1}$ 3474 (strong), 3389 (strong), 2214-2228 (weak, cyano), 1699 (strong, CO stretch), 1381 (strong, C-N stretch) (**Supplementary Figure 13**). ^1H NMR (400 MHz, DMSO- D_6) δ_{H} 8.60 (s, 1H), 8.14 – 8.05 (m, 2H), 8.01 – 7.93 (m, 2H), 7.91 (d, $J = 10.8$ Hz, 1H), 7.58 – 7.47 (m, 4H), 7.42 (s, 1H), 7.38 – 7.25 (m, 2H), 7.19 (dd, $J = 11.8$, 0.8 Hz, 1H) (**Supplementary Figure 8, 9**); ^{13}C NMR (101 MHz, DMSO- D_6) δ_{C} 161.94, 151.13, 143.29, 131.92, 131.01, 129.67, 129.20, 128.80, 128.49, 126.43, 125.24, 124.90, 115.07, 108.58 (**Supplementary Figure 10, 11**).

Conclusion

Photochemical synthesis of (2*E*,4*Z*)-5-(anthracen-9-yl)-2-cyanopenta-2,4-dienamide (**4**) from (2*E*,4*E*)-5-(anthracen-9-yl)-2-cyanopenta-2,4-dienamide using 475 nm can be obtained with a maximum of 87% conversion. Obtaining pure **4** (> 99%) was achieved by precipitating a solution of crude **4** from aqueous SDS and filtering out an acicular crystal of **4**.

Supplementary Materials: This section contains ^1H NMR, ^{13}C NMR, IR, UV-Vis, and HPLC data

Author Contributions: ROK synthesized and characterized the compound. RM determined the MP of the compounds. II interpreted the NMR of the compounds, CJB proofread the manuscript.

Funding:

Acknowledgments: The authors like to acknowledge the continued support of the college of science and health professions at KSAU-HS and the KAIMRC at the Ministry of National Guard Health Affairs.

Conflicts of Interest: The authors declare no conflict of interest.

References

- Kim, T.; Zhu, L.; Al-Kaysi, R.O.; Bardeen, C.J. Organic Photomechanical Materials. *ChemPhysChem* **2014**, *15*, 400–414, doi:10.1002/cphc.201300906.
- Dest, I.T.; Chizhik, S.A.; Sidelnikov, A.A.; Karothu, D.P.; Boldyreva, E. V.; Naumov, P. Mechanically Responsive Crystals: Analysis of Macroscopic Strain Reveals “Hidden” Processes. *J. Phys. Chem. A* **2020**, *124*, 300–310, doi:10.1021/acs.jpca.9b10365.
- Gately, T.J.; Sontising, W.; Easley, C.J.; Islam, I.; Al-Kaysi, R.O.; Beran, G.J.O.; Bardeen, C.J. Effect of Halogen Substitution on

- Energies and Dynamics of Reversible Photomechanical Crystals Based on 9-Anthracenecarboxylic Acid. *CrystEngComm* **2021**, 23, 5931–5943, doi:10.1039/d1ce00846c. 162
163
4. Tong, F.; Chen, S.; Li, Z.; Liu, M.; Al-Kaysi, R.O.; Mohideen, U.; Yin, Y.; Bardeen, C.J. Crystal-to-Gel Transformation Stimulated by a Solid-State E→Z Photoisomerization. *Angew. Chemie - Int. Ed.* **2019**, 58, 15429–15434, doi:10.1002/anie.201907454. 164
165
166
5. Kim, T.; Al-Muhanna, M.K.; Al-Suwaidan, S.D.; Al-Kaysi, R.O.; Bardeen, C.J. Photoinduced Curling of Organic Molecular Crystal Nanowires. *Angew. Chemie - Int. Ed.* **2013**, 52, 6889–6893, doi:10.1002/anie.201302323. 167
168
6. Tong, F.; Xu, W.; Al-Haidar, M.; Kitagawa, D.; Al-Kaysi, R.O.; Bardeen, C.J. Photomechanically Induced Magnetic Field Response by Controlling Molecular Orientation in 9-Methylanthracene Microcrystals. *Angew. Chemie - Int. Ed.* **2018**, 57, 7080–7084, doi:10.1002/anie.201802423. 169
170
171
7. Tong, F.; Kitagawa, D.; Bushnak, I.; Al-Kaysi, R.O.; Bardeen, C.J. Light-Powered Autonomous Flagella-Like Motion of Molecular Crystal Microwires. *Angew. Chemie - Int. Ed.* **2021**, 60, 2414–2423, doi:10.1002/anie.202012417. 172
173
8. Al-Kaysi, R.O.; Bardeen, C.J. Reversible Photoinduced Shape Changes of Crystalline Organic Nanorods. *Adv. Mater.* **2007**, 19, 1276–1280, doi:10.1002/adma.200602741. 174
175
9. Zhu, L.; Tong, F.; Zaghoul, N.; Baz, O.; Bardeen, C.J.; Al-Kaysi, R.O. Characterization of a P-Type Photomechanical Molecular Crystal Based on the: E → Z Photoisomerization of 9-Divinylanthracene Malonitrile. *J. Mater. Chem. C* **2016**, 4, 8245–8252, doi:10.1039/c6tc02517j. 176
177
178
10. Tong, F.; Al-Haidar, M.; Zhu, L.; Al-Kaysi, R.O.; Bardeen, C.J. Photoinduced Peeling of Molecular Crystals. *Chem. Commun.* **2019**, 55, 3709–3712, doi:10.1039/c8cc10051a. 179
180
11. Al-kaysi, R.O. Spontaneous Peeling of Tetragonal Microcrystals with Short Pulses of UV-Light 2019. 181
12. Dong, X.; Tong, F.; Hanson, K.M.; Al-Kaysi, R.O.; Kitagawa, D.; Kobatake, S.; Bardeen, C.J. Hybrid Organic-Inorganic Photon-Powered Actuators Based on Aligned Diarylethene Nanocrystals. *Chem. Mater.* **2019**, 31, 1016–1022, doi:10.1021/acs.chemmater.8b04568. 182
183
184
13. Tong, F.; Xu, W.; Guo, T.; Lui, B.F.; Hayward, R.C.; Palfy-Muhoray, P.; Al-Kaysi, R.O.; Bardeen, C.J. Photomechanical Molecular Crystals and Nanowire Assemblies Based on the [2+2] Photodimerization of a Phenylbutadiene Derivative. *J. Mater. Chem. C* **2020**, 8, 5036–5044, doi:10.1039/c9tc06946a. 185
186
187
14. Jagtap, S. Heck Reaction—State of the Art. *Catalysts* **2017**, 7, doi:10.3390/catal7090267. 188
15. Battistuzzi, G.; Cacchi, S.; Fabrizi, G. An Efficient Palladium-Catalyzed Synthesis of Cinnamaldehydes from Acrolein Diethyl Acetal and Aryl Iodides and Bromides. *Org. Lett.* **2003**, 5, 777–780, doi:10.1021/ol034071p. 189
190
16. Bigi, F.; Carloni, S.; Ferrari, L.; Maggi, R.; Mazzacani, A.; Sartori, G. Clean Synthesis in Water. Part 2: Uncatalysed Condensation Reaction of Meldrum's Acid and Aldehydes. *Tetrahedron Lett.* **2001**, 42, 5203–5205, doi:10.1016/S0040-4039(01)00978-9. 191
192
193
17. Knoevenagel, E. Condensation von Malonsäure Mit Aromatischen Aldehyden Durch Ammoniak Und Amine. *Berichte der Dtsch. Chem. Gesellschaft* **1898**, 31, 2596–2619, doi:10.1002/cber.18980310308. 194
195
18. van Beurden, K.; de Koning, S.; Molendijk, D.; van Schijndel, J. The Knoevenagel Reaction: A Review of the Unfinished Treasure Map to Forming Carbon–Carbon Bonds. *Green Chem. Lett. Rev.* **2020**, 13, 85–100, doi:10.1080/17518253.2020.1851398. 196
197
19. Mukhopadhyay, C.; Datta, A. A Simple, Efficient and Green Procedure for the Knoevenagel Condensation of Aldehydes with N-Methylpiperazine at Room Temperature under Solvent-Free Conditions. *Synth. Commun.* **2008**, 38, 2103–2112, doi:10.1080/00397910802029364. 198
199
200
20. Nanowires, M.; Al-kaysi, R.O.; Al-suwaidan, S.D.; Bardeen, C.J.; Kim, T.; Al-muhanna, M.K. Photo-Induced Spontaneous Coiling and Bending Of. In Proceedings of the International Conference on Nanotechnology: Fundamentals and Applications 2013; 2013; pp. 1–7. 201
202
203

-
21. Reddy, M.J.R.; Kumar, P.A.; Srinivas, U.; Reddy, V.V.; Reddy, M.J.R.; Rao, G.V.; Rao, V.J. *Wavelength Dependent Regioselective E→Z Isomerization of 9-Anthryldiene Derivatives*; 2007; Vol. 46;. 204
205
22. Tong, F.; Liu, M.; Al-Kaysi, R.O.; Bardeen, C.J. Surfactant-Enhanced Photoisomerization and Photomechanical Response in Molecular Crystal Nanowires. *Langmuir* **2018**, *34*, 1627–1634, doi:10.1021/acs.langmuir.7b03848. 206
207
23. Zhou, W.; Li, H. bo; Xia, C. nian; Zheng, X. ming; Hu, W. xiao The Synthesis and Biological Evaluation of Some Caffeic Acid Amide Derivatives: E-2-Cyano-(3-Substituted Phenyl)Acrylamides. *Bioorganic Med. Chem. Lett.* **2009**, *19*, 1861–1865, doi:10.1016/j.bmcl.2009.02.081. 208
209
210
211
212
213
214
215
216
217
218
219
220
221
222
223
224
225
226
227
228
229
230
231
232
233
234
235
236
237
238
239
240
241
242
243
244
245
246
247
248
249
250
251
252
253
254
255
256
257
258

Supplementary Material

259

260

(2E,4Z)-5-(anthracen-9-yl)-2-cyanopenta-2,4-dienamide

261

Rabih O. Al-Kaysi ^{1,*}, Imadul Islam ¹, Raghad Al-Muzarie ¹, and Christopher J. Bardeen ²

262

263

264

265

266

267

268

269

270

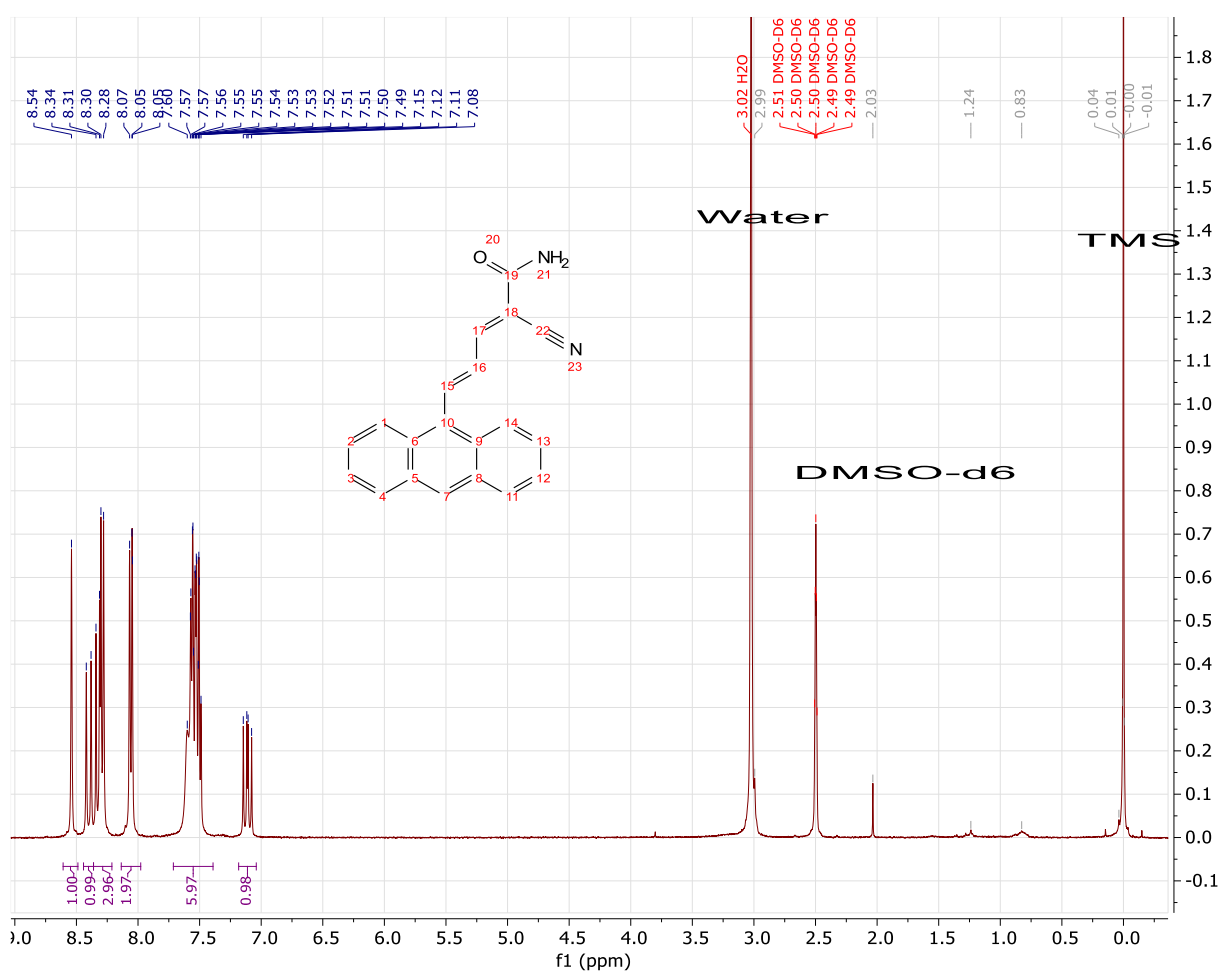
271

272

273

274

275

Supplementary Figure 1: ¹H NMR of **3** in 33% (V/V) DMSO-d₆ in CCl₄

276

277

278

279

280

281

282

283

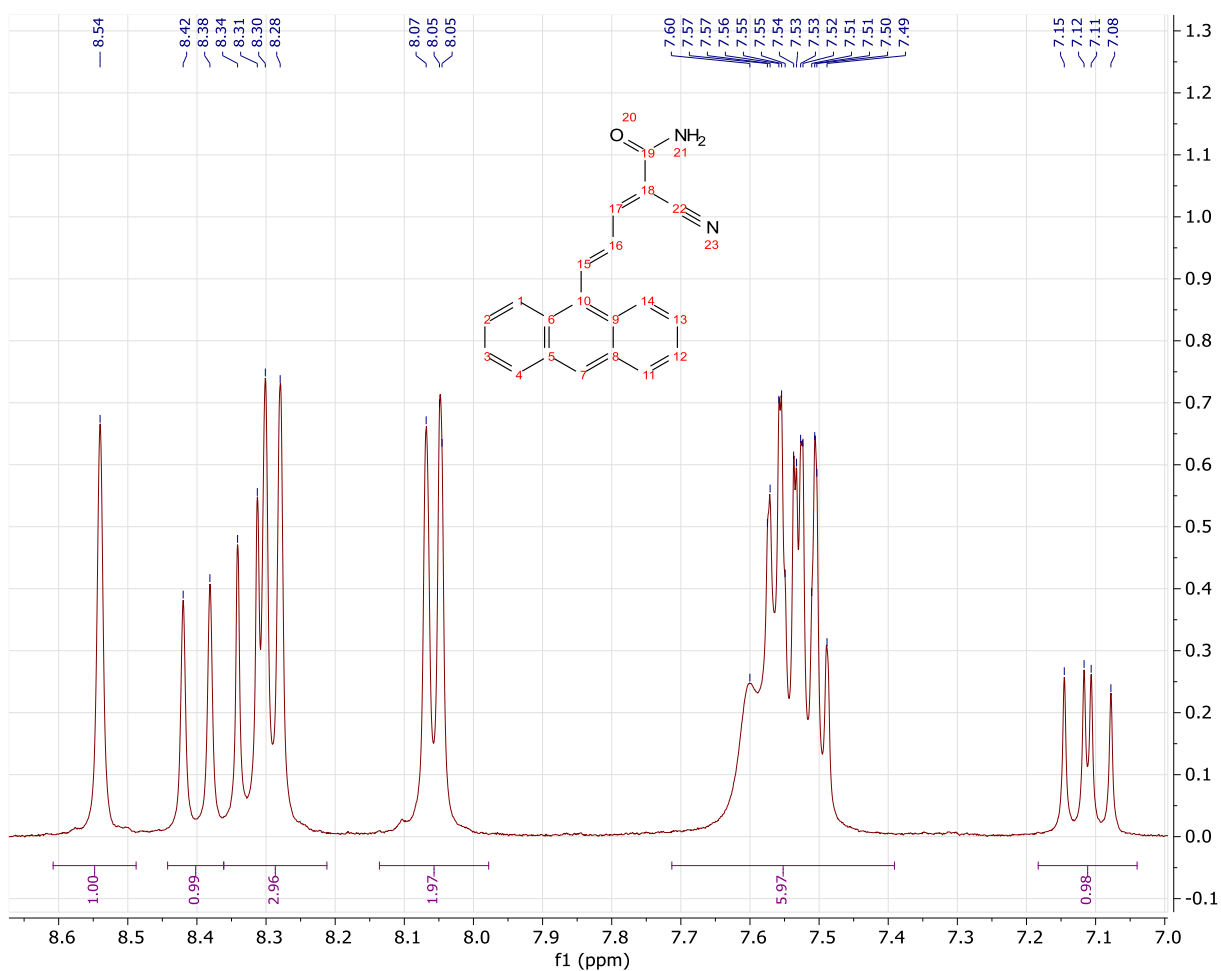
284

285

286

287

288



Supplementary Figure 2: ¹H NMR of **3** in 33% (V/V) DMSO-d₆ in CCl₄, zoomed into the region between 8.6-7.0 ppm

289

290

291

292

293

294

295

296

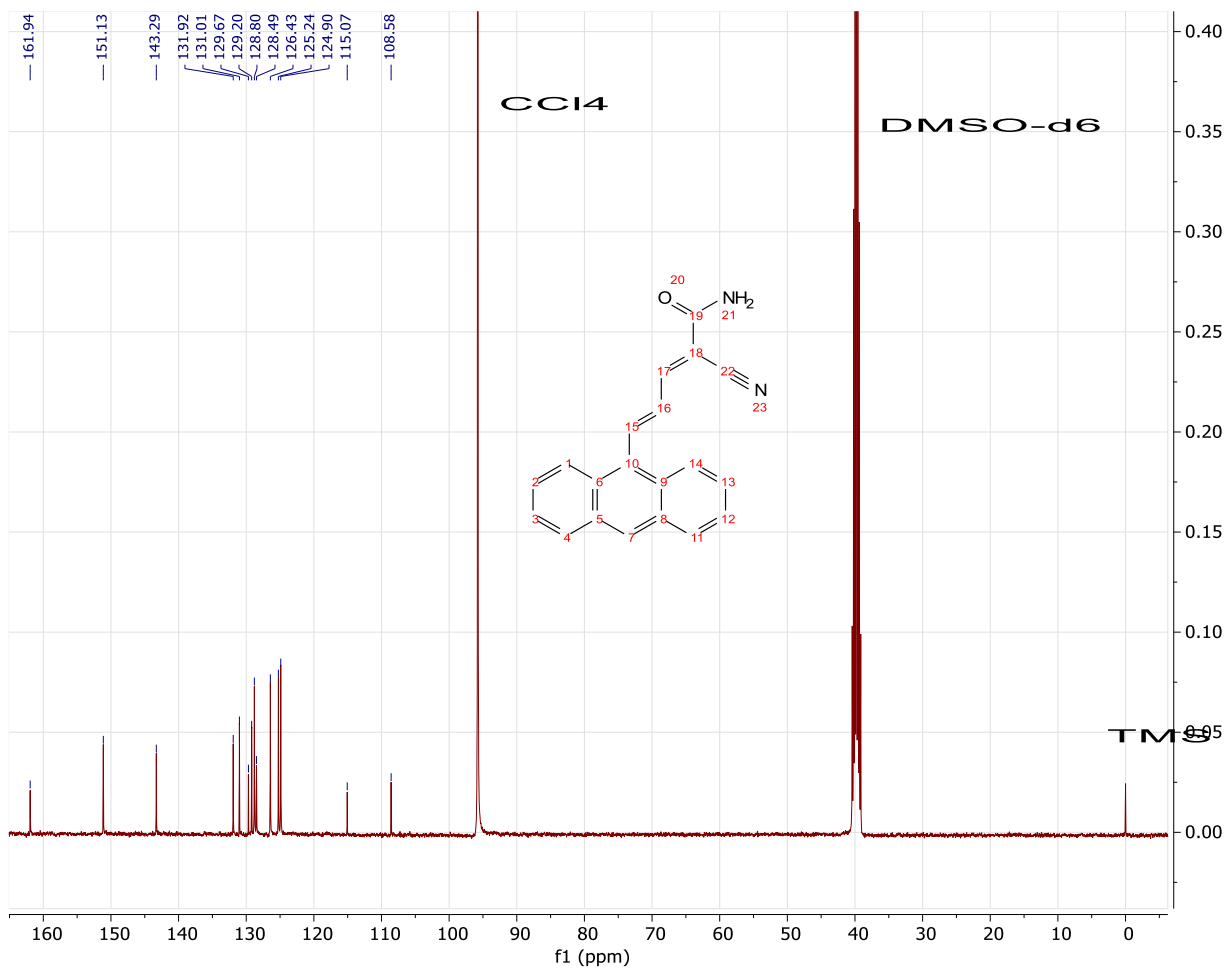
297

298

299

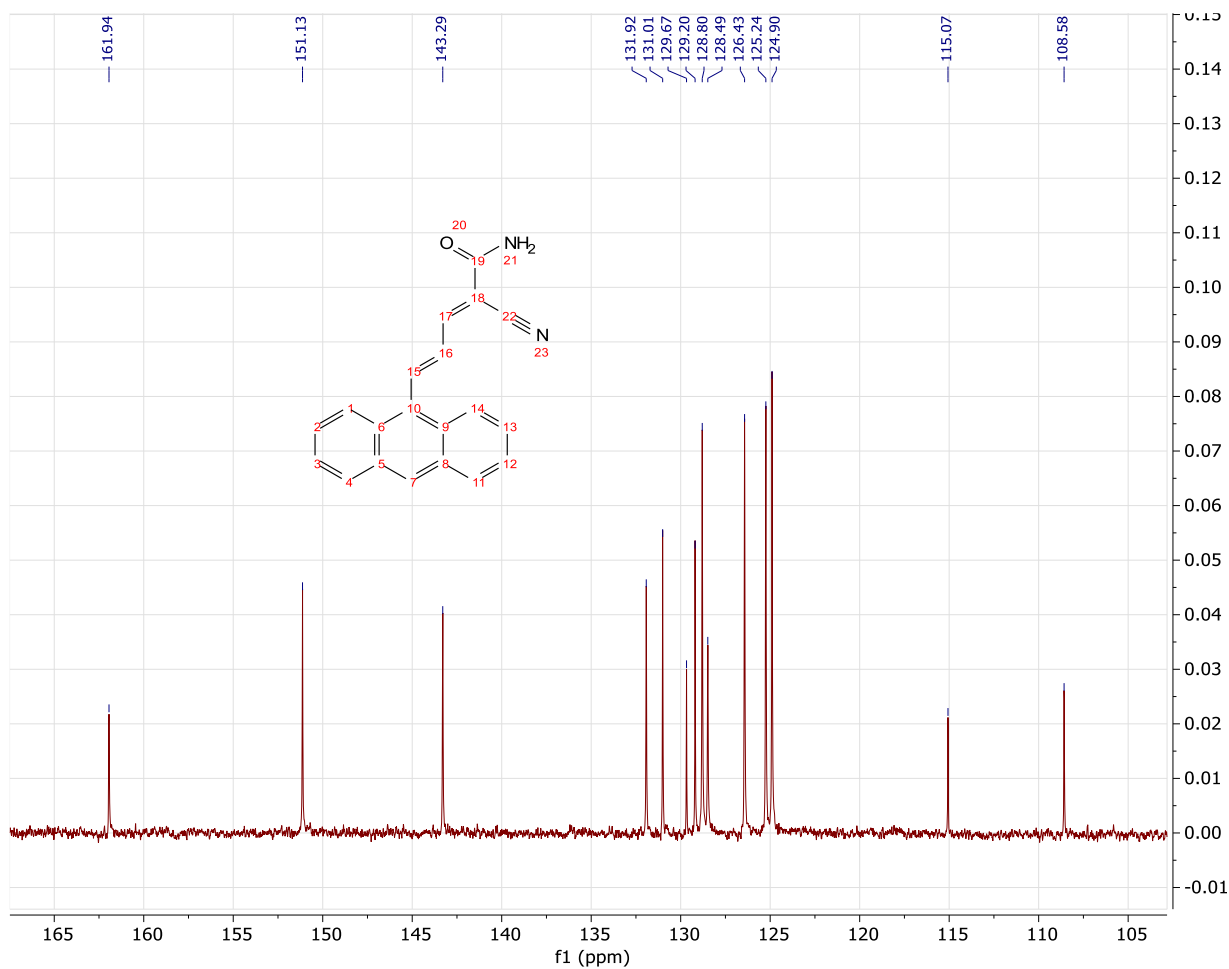
300

301



Supplementary Figure 3: ¹³C NMR of **3** in 33% (V/V) DMSO-d₆ in CCl₄.

315



316

Supplementary Figure 4: ^{13}C NMR of **3** in 33% (V/V) DMSO- d_6 in CCl_4 . Zoomed in to the region between 165-105 ppm

317

318

319

320

321

322

323

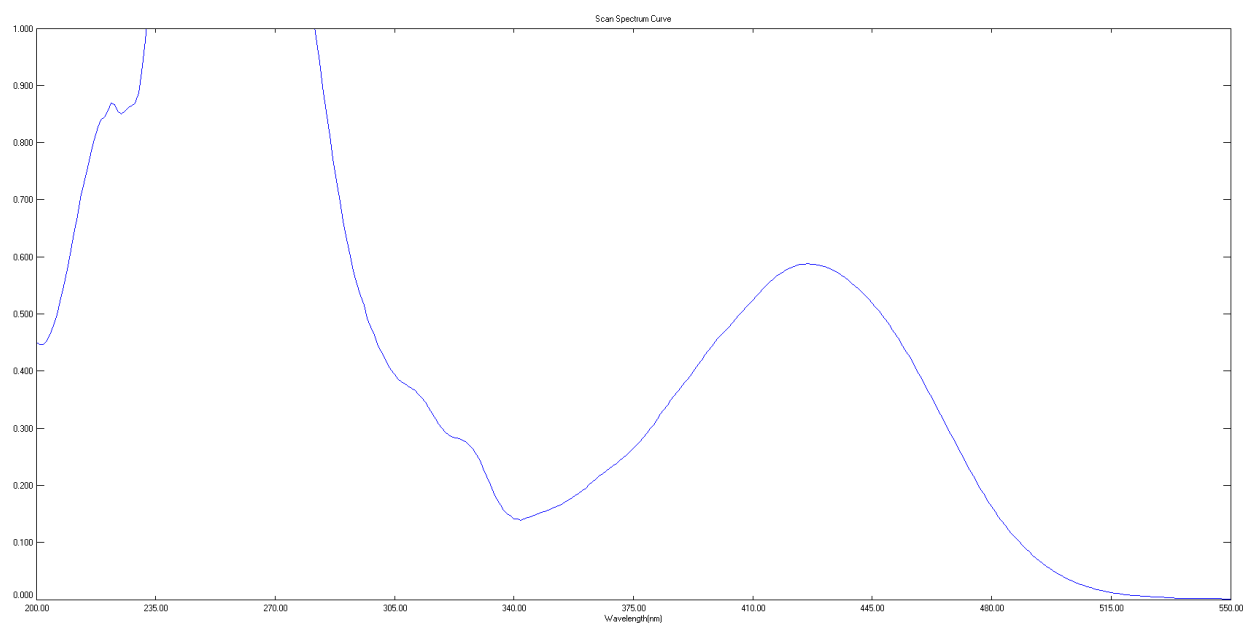
324

325

326

327

328



329

Supplementary Figure 5: UV-Vis absorption spectrum of **3** in CH₃CN

330

331

332

333

334

335

336

337

338

339

340

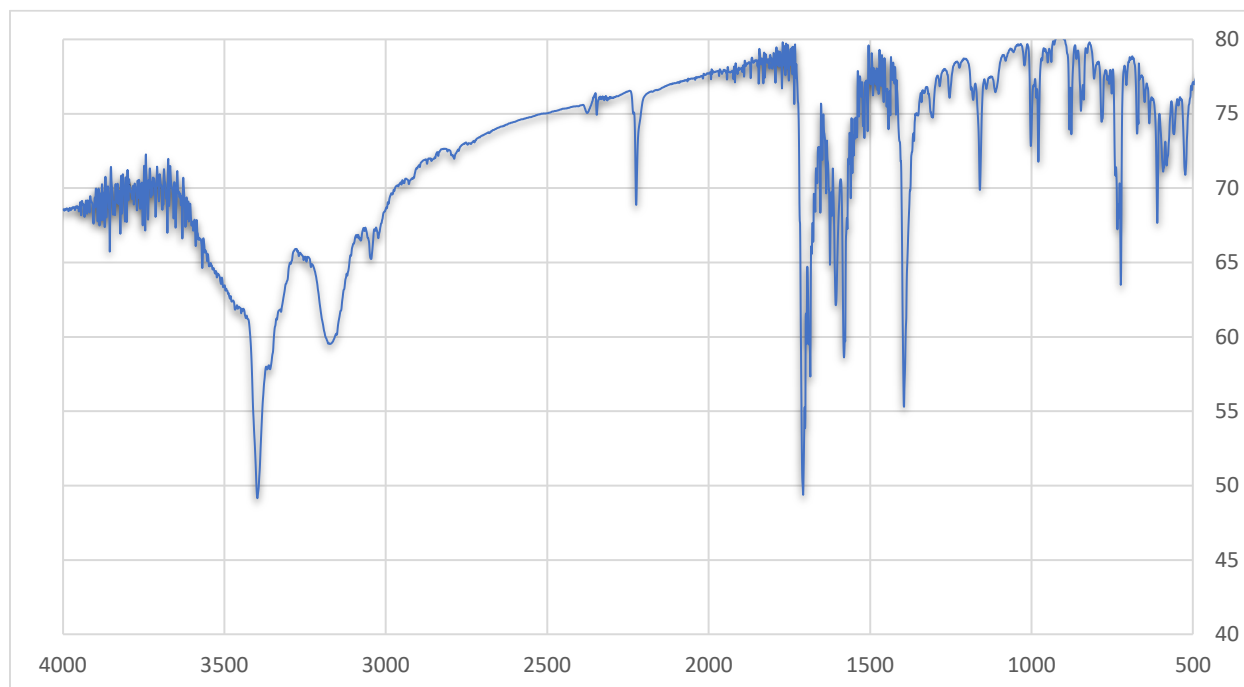
341

342

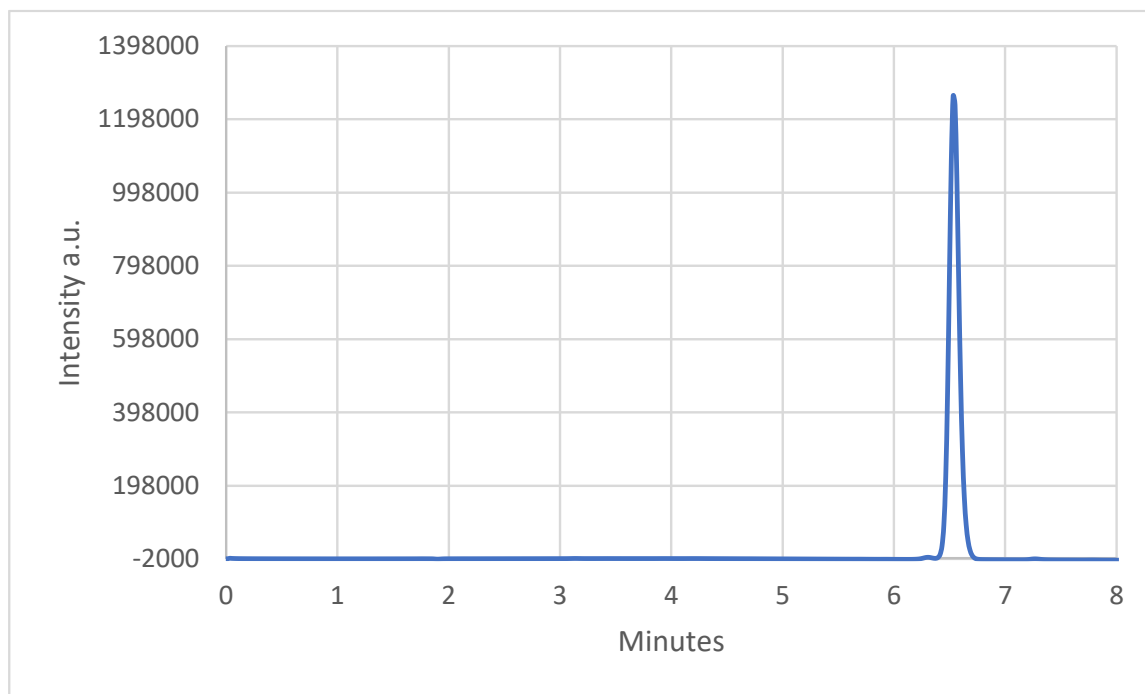
343

344

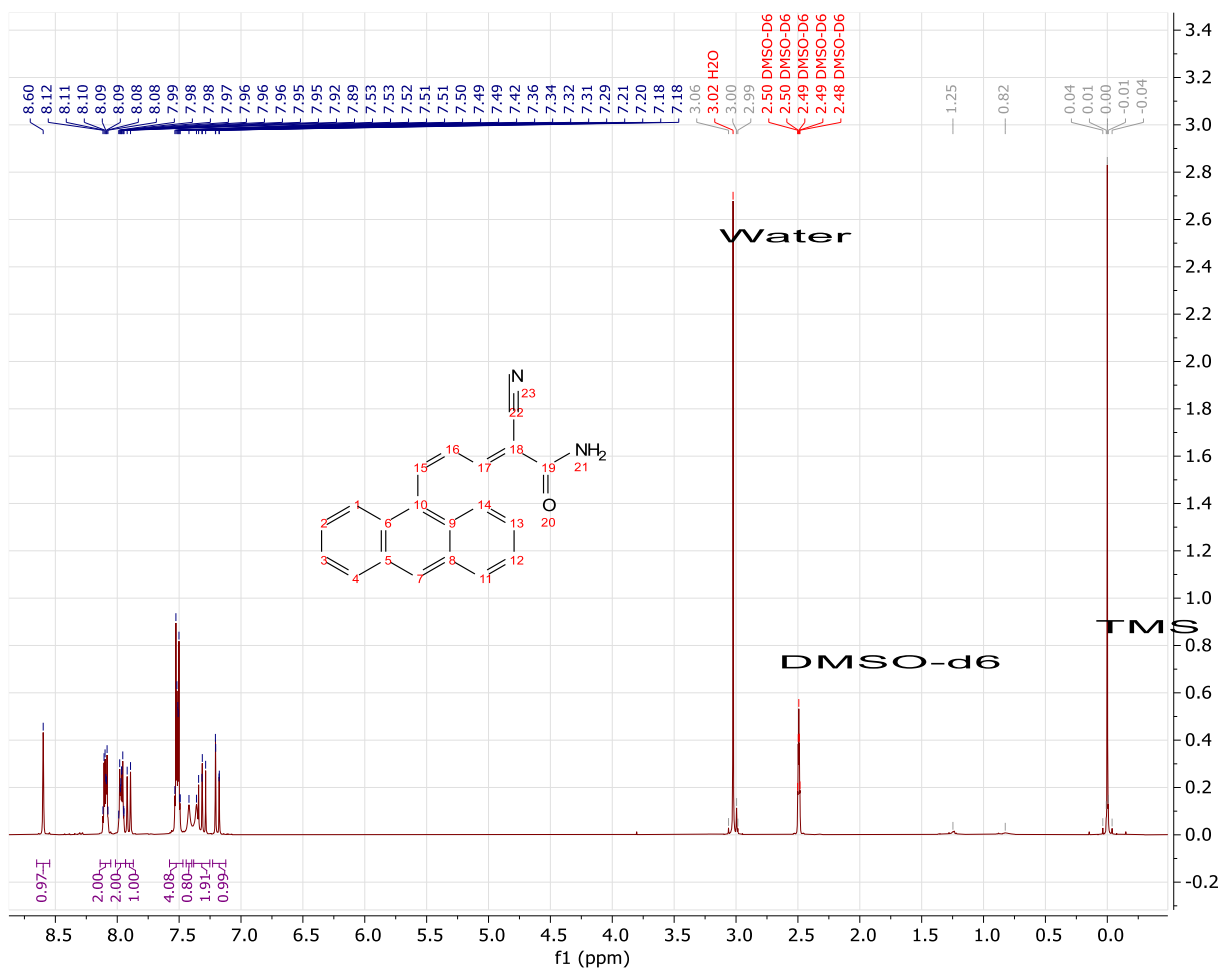
345

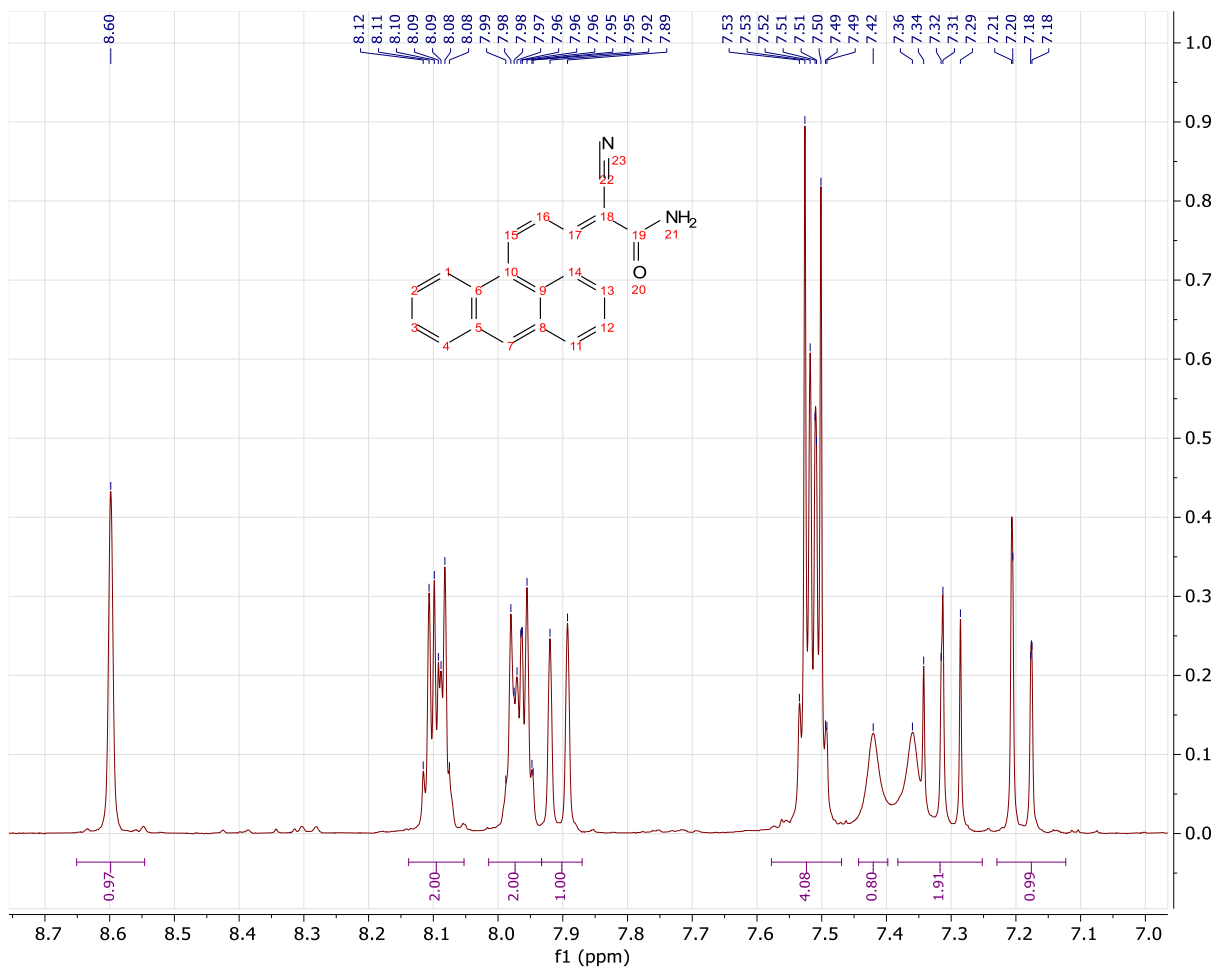


Supplementary Figure 6: IR spectrum of **3** in mixed with KBr and pressed into a pellet.



Supplementary Figure 7: HPLC chromatogram of **3** with elution time 6.52 minutes

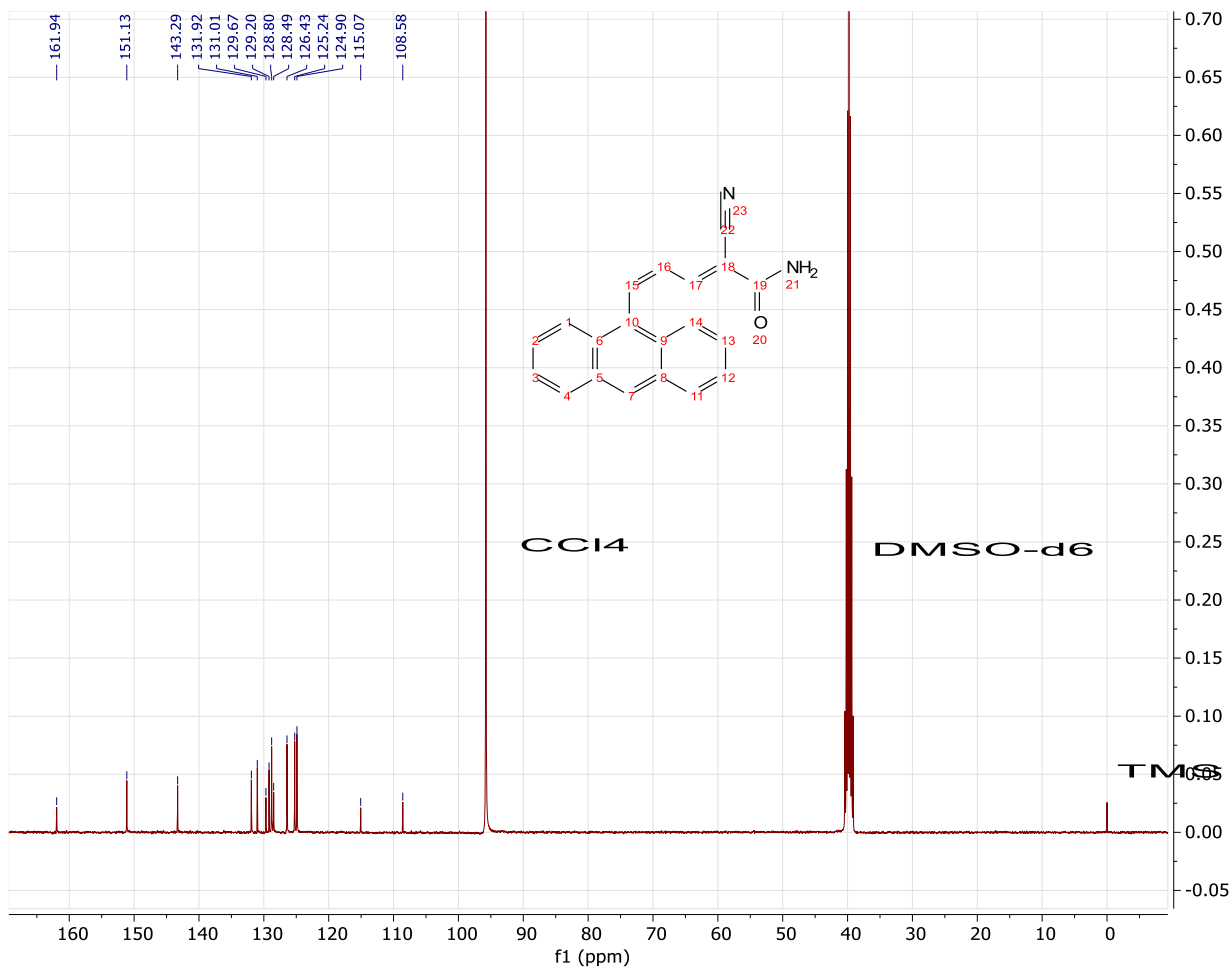
Supplementary Figure 8: ¹H NMR of 4 in 33% (v/v) DMSO-d₆ in CCl₄.



Supplementary Figure 9: ^1H NMR of **4** in 33% (V/V) DMSO- d_6 in CCl_4 . Zoomed in to the region between 8.7-7.1 ppm

408

409



410

Supplementary Figure 10: ¹³C NMR of 4 in 33% (V/V) DMSO-d₆ in CCl₄.

411

412

413

414

415

416

417

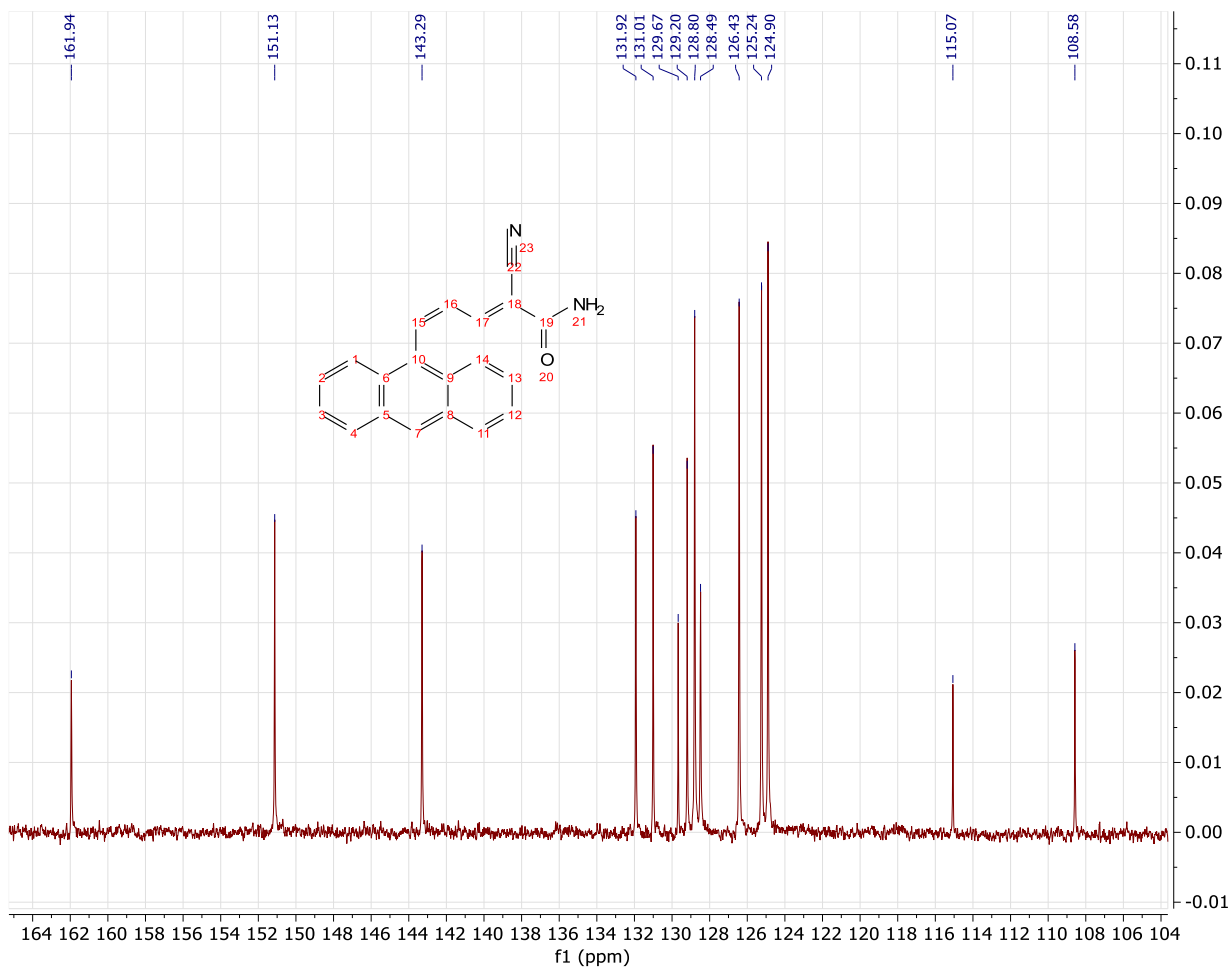
418

419

420

421

422



423

Supplementary Figure 11: ^{13}C NMR of **4** in 33% (V/V) DMSO- d_6 in CCl_4 . . Zoomed into the region between 164-106 ppm

424

425

426

427

428

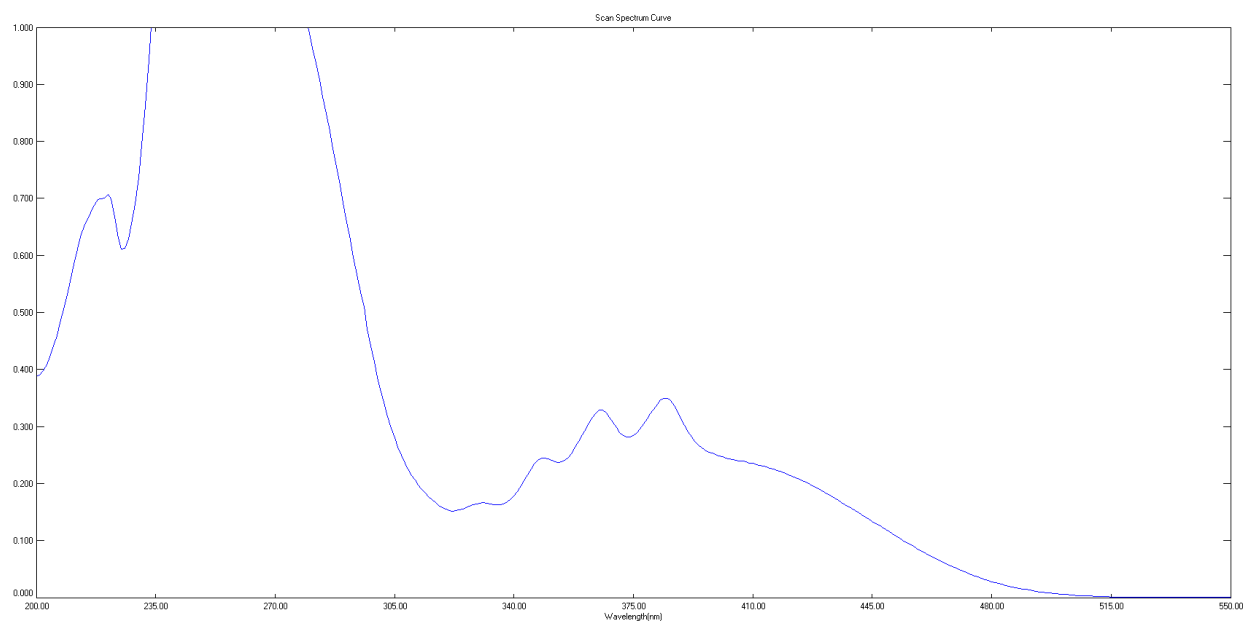
429

430

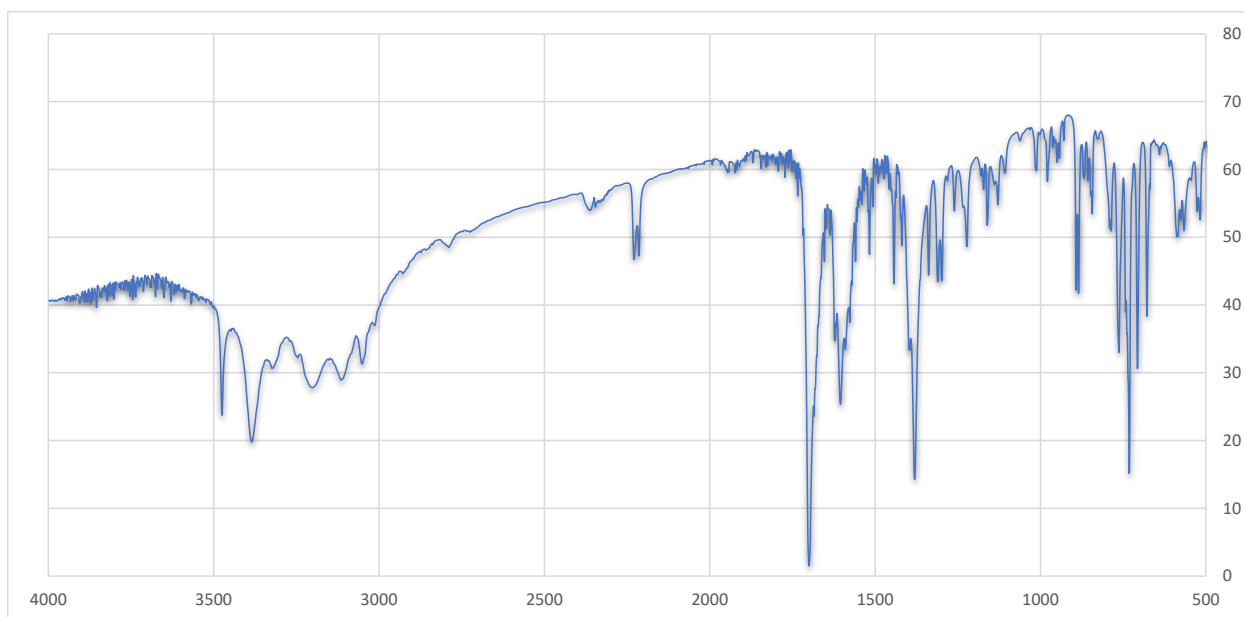
431

432

433



Supplementary Figure 12: UV-Vis absorption spectrum of **4** in CH₃CN



Supplementary Figure 13: IR spectrum of **4** in mixed with KBr and pressed into a pellet.

448

449

450

451

452

453

454

455

456

457

458

459

460

461

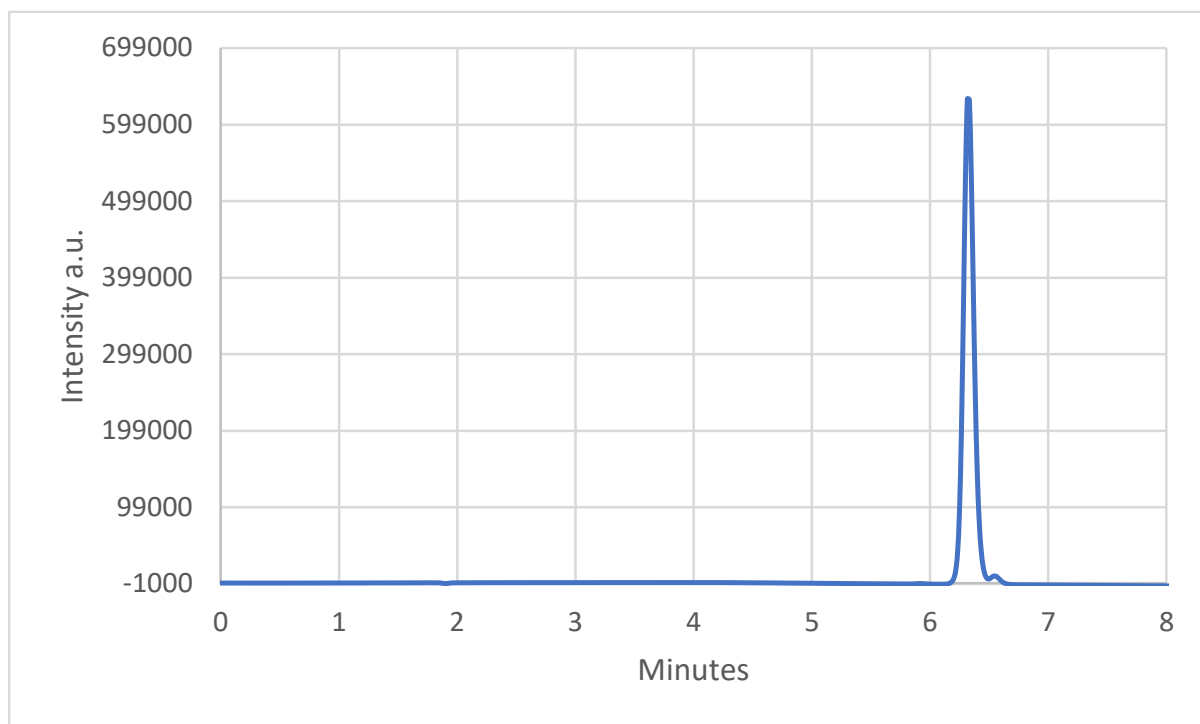
462

463

464

465

466



467

Supplementary Figure 14: HPLC chromatogram of **4** with elution time 6.28 minutes

468

469

470

471

472

473

474

475

476

477

478

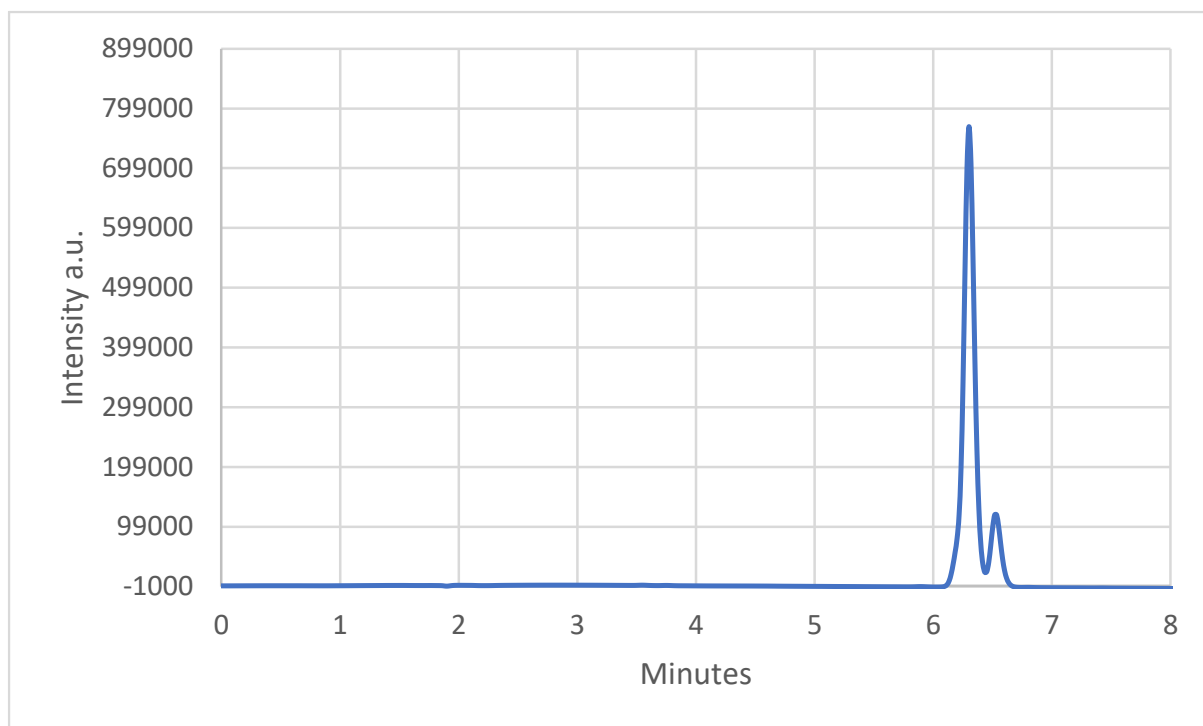
479

480

481

482

483



484

Supplementary Figure 15: HPLC chromatogram after photolysis of **3** in acetonitrile using blue-light LEB. Composition is 87% of compound **4** (left large peak) and 13% unconverted **3** (smaller peak)

485

486

487

488

489

490

491

492

493

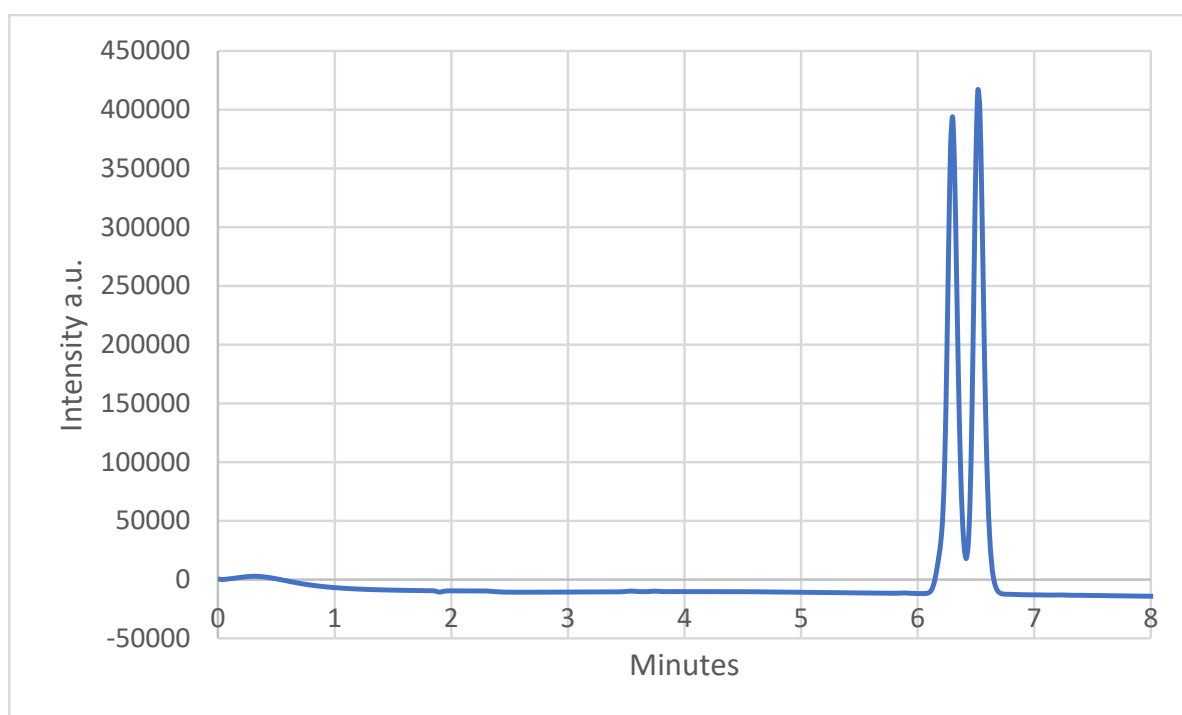
494

495

496

497

498



Supplementary Figure 16: HPLC chromatogram after photolysis of **4** in acetonitrile using 365 nm light. The final composition is 45% of compound **4** (left large peak) and 55% **3** (smaller peak). Photochemical reversibility of **3** and **4**

499

500

501

502

503

504

505

506

507

508

509

510

511

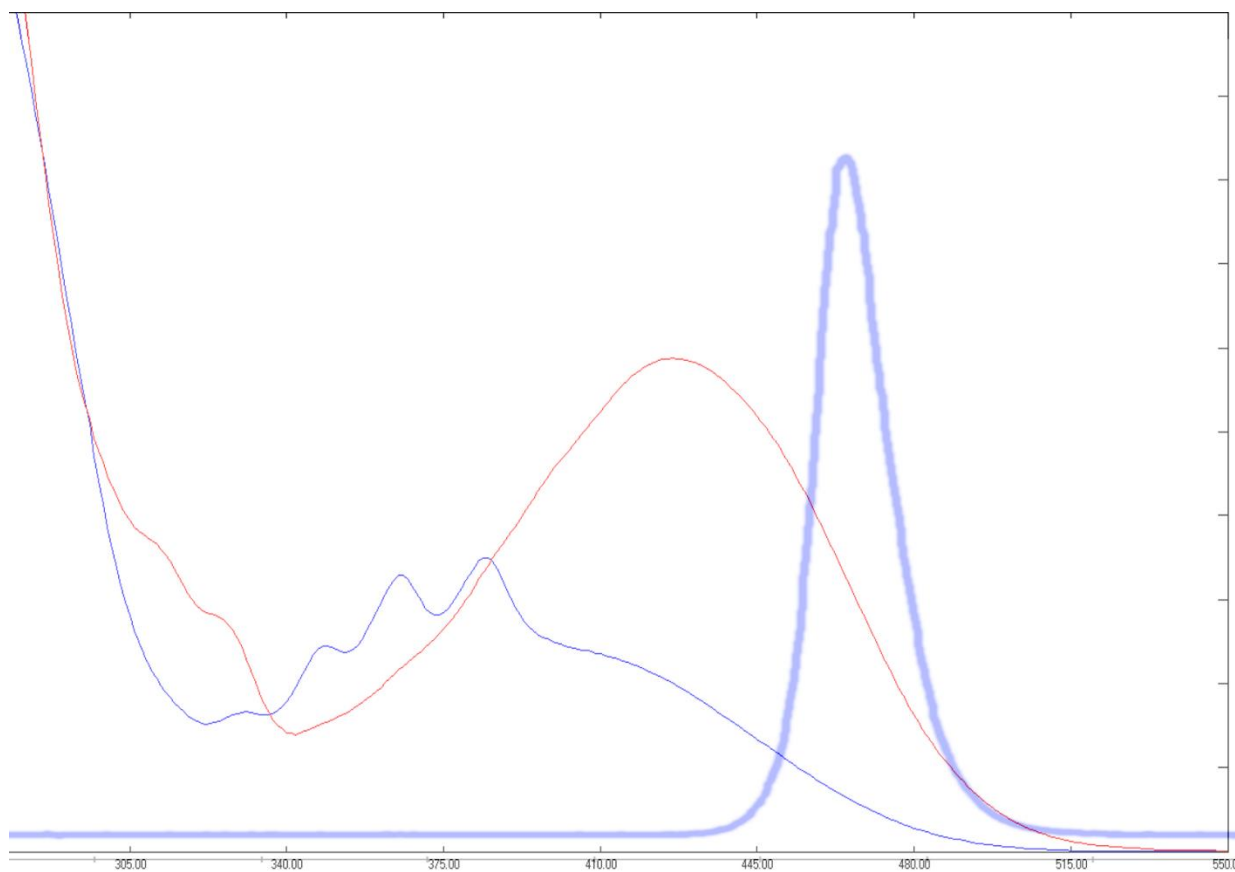
512

513

514

515

516



Supplementary Figure 17: UV-Vis absorption spectra with relative extinction values of **4** (thin blue line) and **3** (thin red line). The broad cyan-colored curve is the emission spectrum of the LED light source used.